Technical note:

**On the interface shear resistance of a novel geogrid with in-plane drainage capability**

**Brendan C. O'Kelly and Patrick J. Naughton**

Brendan C. O'Kelly (corresponding author)
Lecturer in Civil Engineering,
Department of Civil, Structural and Environmental Engineering,
Museum Building, Trinity College Dublin, Dublin 2, Ireland.
Tel. 00353 1896 2387; Fax. 00353 1677 3072; E-mail bokelly@tcd.ie

Patrick J. Naughton
Lecturer,
School of Engineering,
Institute of Technology, Sligo,
Ballinode, Sligo, Ireland.
Tel. 00353 71915 5489; Fax. 00353 71915 5390; E-mail naughton.patrick@itsligo.ie

Published in the Journal of Geotextiles and Geomembranes, 2008, Vol. 26, No. 4, 357–362.

## Abstract

The enhancement in the short-term interface shear strength (critical case for embankment construction) achieved by a novel geogrid that combines both reinforcement and in-plane drainage functions was studied. Marginal fill (wet gravely clay) was standard Proctor compacted to 92% of its maximum dry density and tested under consolidated-undrained conditions in the large shearbox apparatus. The interface shear resistance ($\tau_{s\text{-}g}$) values mobilized for the novel geogrid were similar to the undrained shear strength of the surrounding soil. In contrast, the $\tau_{s\text{-}g}$ values mobilized for a conventional geogrid, which had similar physical and tensile strength properties, were only between 82 and 85% of the undrained shear strength of the soil. Overall, the undrained shear resistance mobilized along the soil-geogrid interface was between 20 and 30% greater for the novel geogrid than for the conventional geogrid.

*Keywords;* Drainage; Dual function; Geogrid; Interface; Marginal fill; Shear resistance

## 1. Introduction

Geosynthetics are widely used in reinforced-earth and landfill construction and soft ground improvement (Bergado et al., 2006; Long et al., 2007; Tatsuoka et al, 2007; Rowe and Taechakumthorn, 2008), and have many advantages including speed of construction, flexibility and durability, use of local readily-available soils rather than imported quarry product, and cost effectiveness. More recently, innovative dual-function geosynthetics that combine both reinforcement and drainage functions have been developed (Kempton et al., 2000; Bergado et al., 2002; Lorenzo et al., 2004; Zornberg and Kang, 2005), which can facilitate the use of marginal fill in the construction of reinforced earth structures. Marginal fill is defined as predominantly granular material that includes high silt and/or clay fractions (more than 15% by dry weight passing the 0.063-mm sieve) and often has high water content, with typically only 90 to 95% of its maximum dry density achieved under standard Proctor compaction. Dual function geosynthetics included in the earth structures provide reinforcement and preferential drainage channels, thereby increasing the factor of safety against slope instability.

The use of geosynthetics requires a proper understanding of the soil-geosynthetic interaction mechanisms. Utilizing marginal fill would involve considerable savings (Lorenzo et al., 2004) on condition that the intended engineering purpose can be achieved. However, most of the previous research has studied the interaction parameters (pullout resistance and shear stress–strain characteristics) between geosynthetics and granular soils. Few studies have been carried out in relation to the interaction parameters between cohesive soils and geosynthetics (Bergado et al., 1991; Nagahara et al., 2004; Almohd et al., 2006; Long et al. 2007). For example, the angle of interface friction value for conventional geogrids is lower than the angle of shearing resistance of the surrounding soil, and this must be considered in analyzing the factor of safety on slope instability where potential slip surfaces can align with the soil-geosynthetic interface. This paper presents a laboratory study into the short-term interface shear resistance ($\tau_{s\text{-}g}$generally critical case) achieved for using a novel dual- function geogrid in the construction of earth embankments using wet cohesive fill.

## 2. Materials

### *2.1 Test soil*

The test soil was Brown Dublin Boulder clay (Skipper et al., 2005; Long and Menkiti, 2007); a gravely clay of low plasticity (liquid limit of 31%; plastic limit of 16% and plasticity index of 15%). The test material had a natural water content value of about 11% and a specific gravity of solids value of 2.70. Standard Proctor compaction tests indicated a maximum dry density of 1.84 tonne/m$^3$ at an optimum water content for compaction value of 13.0%.

### *2.2 Geogrids*

The novel geogrid (Paradrain$^{TM}$) comprised two elements, namely: (i) flexible reinforcement straps that had been profiled to provide in-plane drainage channels; (ii) a drainage element (non-woven geotextile that had been bonded to the shoulders of the drainage channels (Fig. 1). The reinforcement straps (75-mm pitch in the reinforcing direction and 33-mm wide and 2.5-mm thick in cross-section) comprised polyester fibres that were enclosed in a smooth polyethylene sheath, with a characteristic tensile strength of 150 kN/m (main reinforcement). Previous research by Kempton et al. (2000) and Zornberg and Kang (2005) on the performance of the novel geogrid in wet gravely clay and English China clay indicated that the $\tau_{s\text{-}g}$ values mobilised under low to medium applied normal stresses was generally 30% greater than that mobilized for a conventional geogrid with similar tensile strength properties. It should be noted that there are other available products which serve both reinforcement and drainage functions.

A conventional, smooth biaxial geogrid (Paragrid$^{TM}$), which had the same physical and tensile strength properties as the novel geogrid, was also tested in the shearbox apparatus as a basis for comparison. Further details on the properties of these geosynthetics have been reported by Kempton et al. (2000); Zornberg and Kang (2005) and the manufacturer, Linear Composites Limited (2007).

## 3. Experimental method

### *3.1 Test program*

Consolidated undrained (CU) shearbox tests were conducted using the large shearbox (300 by 300 mm in plan, and 150 mm in depth) in accordance with ASTM D5321 (2002) to measure the development of the shear resistance under medium to high applied normal stresses. The CU shearbox tests simulated in the geotechnical laboratory the sequence whereby the fill material is placed and compacted in stages onsite, with consolidation occurring during the intervening periods. The test program included:

- Five tests on the soil alone;
- Five tests shearing the soil over the conventional geogrid;
- Five tests shearing the soil over the novel geogrid;
- Five tests shearing the soil over a smooth aluminium plate.

### *3.2 Specimen preparation*

The geogrid specimens were attached to a smooth aluminium plate (300 by 300 mm in plan), which had been located flush with the shear plane, at the mid-height of the shearbox, with the main reinforcement aligned in the direction of shear (Fig. 2). Both sets of geogrid specimens were essentially fully fixed (bonded to the aluminium plate using water-proof adhesive and with one end also fixed to the plate using three screw fasteners) preventing elongation of the geogrid. The novel geogrid was secured such that its drainage (geotextile) strips were in contact with the soil, which was contained in the upper half of the shearbox. The fasteners were necessary in all of the tests since the geogrids became detached during the shearing stage when adhesive alone had been used to form the bond.

The reinforcement straps of the novel and conventional geogrids covered about 56 and 58%, respectively, of the plate surface area (greater than the 50% area coverage recommended by Koerner (1998) for this set up. The soil was in direct contact with the aluminium plate over the remaining 44 and 42% of the surface areas, respectively. New geogrid specimens were prepared and secured to the aluminium plate at the start of each test.

The test soil was disaggregated to pass the 20-mm sieve size and the larger-sized solid particles, which accounted for about 11% of the bulk mass, were removed. The soil was wetted, increasing its water content to about 16.5% (i.e. water content 3.5% greater than the optimum water content for compaction) and the material was allowed to equilibrate overnight. A know mass of the wet soil was placed and compacted in the upper half of the shearbox in three layers of equal thickness, with each layer being imparted 25 blows of a 75 by 100 mm steel tamper, to obtain a dry density of 1.68 tonne/m$^3$ (92% of the maximum dry density achieved under standard Proctor compaction) and an air voids content of 8%. In this condition, the test soil was categorized as marginal fill. All of the shearbox specimens had the same initial water content.

### *3.3 Shearbox tests*

An axial normal stress was applied via the loading platen in contact with the top of the compacted soil specimen, which was then allowed to consolidate over a period of between 18 and 24 hours. Reinforced-earth embankments are typically between 5 and 10 m in height so that the different interfaces were tested under applied normal stresses in the range of 111 to 222 kPa.

The consolidation properties of the soil could not be determined by applying standard curve-fitting techniques to the measured compression versus time responses (Fig. 3) since the soil was in a partially saturated condition ($S_r \cong 78\%$). A relatively large initial settlement of about 5 mm was recorded, and largely occurred due to the compression of the pore air voids and also some bedding down of the contact surfaces in the shearbox under the applied normal stress. However, the set up of the specimens ensured that the geogrids (attached to the aluminium plate located at the mid-height of the shearbox) remained aligned with the pre-defined shear plane. Drainage to the pore-air voids, and hence dissipation of the excess pore water pressure generated under the applied stress, would have been substantially complete in the vicinity of the novel geogrid straps by the end of the consolidation period. This has been shown experimentally by Kempton et al. (2000) from measurements of the excess pore water pressure response during dissipation and pullout tests on the novel geogrid embedded in English China clay.

The consolidated specimens were then sheared quickly to determine the shear resistance values mobilized over the different interfaces under undrained conditions. The soil in the upper half of the shearbox was displaced at a rate of 0.25 mm/minute relative to the geogrid and aluminium plate, which were both set up flush with shear plane. Koutsourais et al. (1991) and Koerner (1998) have reported that although the soil specimen was in a partially saturated state, this rate of shear displacement was sufficiently quick to produce undrained shear conditions.

## 4. Experimental results and analysis

The shearbox results were analyzed in terms of the total stress condition since the value of the pore pressure during shearing, particularly for the conventional geogrid, was unknown. The shear resistance of all of the interface combinations was found to increase in value with increasing applied stress due to drainage to the pore-air voids, and hence dissipation of the excess pore pressures. Figures 4 and 5 show the mobilized shear resistance versus shear displacement for the soil-aluminium interface ($\tau_{s\text{-}p}$) and the soil itself ($\tau_{s\text{-}s}$). The Mohr-Coulomb failure line of best-fit for the soil alone gave c = 35 kPa and $\phi = 26^o$ (peak values mobilized between 7 and 9% shear strain, Fig. 4(b)); where c is the apparent cohesion and $\phi$ is the angle of shearing resistance (total stress condition). The test soil continued to compress axially, but at a reduced rate, during the shearing stage. Similar analysis of the data for the soil-aluminium interface, based on the $\tau_{s-p}$ values mobilized at 8% strain, gave a = 5 kPa and $\delta = 20^o$; where a is the apparent adhesion and $\delta$ is the angle of interface friction (total stress condition).

Figure 6 shows the mobilized shear resistance versus shear displacement for the soil-geogrid-aluminium plate interfaces ($\tau_{s-p-g}$). The plots exhibited a characteristic shape. Most of the shear resistance had been mobilized by about 9 mm shear displacement (3% shear strain) although the $\tau_{s-p-g}$ value continued to steadily increase, without reaching a peak value, before the tests had to be stopped at the limiting shear displacement of 45 mm (15% strain) for the shearbox apparatus. Similar constitutive behaviour has been reported from pullout tests on the novel geogrid in wet gravely clay by Zornberg and Kang (2005).

Figure 7 shows the undrained interface shear resistance ($\tau_{s-g}$) mobilized for the soil-geogrid combination (more representative of the field condition). The interface resistance values were adjusted using Eq. (1) to take into account that the soil had been in contact with the aluminium plate over 42 to 44% of the shear area during the shearbox tests. The contribution of the interlock between the soil particles and the geogrid reinforcement straps to the mobilised shear resistance was not significant since shearing had occurred along the direction of the main reinforcement in the shearbox tests.

$$\tau_{s-g} = \tau_{s-p-g} + [(\tau_{s-s} - \tau_{s-p})(1 - A_g)] \qquad (1)$$

where $\tau_{s-p-g}$ is the shear resistance mobilized over the soil-plate-geogrid shear plane; $\tau_{s-s}$ is the shear resistance of the soil itself; $\tau_{s-p}$ is the shear resistance mobilized over the soil-aluminium plate and $A_g$ is the fraction of the surface area of the aluminium plate that had been covered by the geogrids.

Figure 8 shows the $\tau_{s-g}$ values mobilized at 5, 7.5 and 10% shear strain for the novel and conventional geogrids. The $\tau_{s-g}$ values have been normalized by the corresponding shear resistance ($\tau_{s-s}$) for the soil. The strain range of between 5 and 10% was chosen since the undrained shear strength of the soil had been fully mobilized by about 8 to 9% shear strain.

In general, the $\tau_{s-g}$ values mobilized for the novel geogrid at 10% shear strain were, for practical purposes, the same as the undrained shear strength of the soil. In contrast, the normalised $\tau_{s-g}$ values were typically only 82% for the conventional geogrid at the same strain level. Figure 8 also shows that the ratio of the $\tau_{s-g}$ to $\tau_{s-s}$ values may be strain level dependent, reducing slightly from typically 85 to 82% with increasing shear strain from 5 to 10%.

Figure 9 shows the mobilized $\tau_{s\text{-}p\text{-}g}$ and $\tau_{s\text{-}g}$ values for the novel geogrid, expressed as a percentage of the conventional geogrid values. Significant increases in the $\tau_{s\text{-}g}$ values (typically between 20 and 25% at 10% shear strain) are achieved by the novel geogrid compared with the conventional geogrid. The increase in the interface shear resistance for the novel geogrid was found to be both stress and strain level dependent; reducing marginally with increasing applied normal stress, and increasing marginally with increasing shear strain (Figs. 8 and 9). The experimental results for the test soil are consistent with the enhancements in the $\tau_{s\text{-}g}$ values reported from pull-out tests on the novel geogrid in wet gravely clay (Zornberg and Kang, 2005) and English China clay (Kempton et al., 2000) at lower applied normal stresses, also plotted in Fig. 9.

## 5. Discussion

The novel geogrid performed considerably better than the conventional geogrid for the marginal cohesive material tested. The experimental results of this and other studies (Kempton et al., 2000; Zornberg and Kang, 2005) have shown that the undrained shear strength ($\tau_{s\text{-}g}$) mobilised along the interface is between 20 and 30% greater for the novel geogrid than for conventional geogrids with similar tensile strength properties. The excess pore water pressures generated in the vicinity of the reinforcement straps of the novel geogrid can rapidly dissipate along its in-plane drainage channels. This has been shown experimentally by Kempton et al. (2000) using dissipation tests on the novel geogrid in English China clay. A higher state of effective stress, and hence a higher shear resistance, is achieved in the immediate vicinity of the shear plane. By reducing the time for primary consolidation to occur, the novel geogrid provides a greater enhancement in the short-term geotechnical stability of earth structures than conventional geogrids. Consequently, wet cohesive fill can be used to safely construct embankments and slopes over a shorter construction period. In contrast, the build up in the excess pore water pressure in the vicinity of the smooth conventional geogrid during shearing, reduces its interface shear capacity in the short-term to between 82 and 85% of the undrained shear strength of the surrounding soil.

## 6. Summary and conclusions

The enhancement in the short-term interface shear strength achieved by a novel geogrid, which combines both reinforcement and in-plane drainage functions, was studied. The test soil was low-plasticity gravely clay that had been compacted to less than 95% of its maximum dry density achieved under standard Proctor compaction, and at a water content that exceeded the optimum water content for compaction by 3.5%.

The interface shear resistance ($\tau_{s\text{-}g}$) values mobilized for the novel geogrid were similar to the undrained shear strength of this marginal fill. The excess pore water pressures in the vicinity of the shear plane dissipated rapidly along the drainage channels in the reinforcement straps, thereby achieving the full shear resistance along the shear plane. In contrast, the $\tau_{s\text{-}g}$ values mobilized for the conventional geogrid, which had similar physical and tensile strength properties, were only between 82 and 85% of the undrained shear strength of the surrounding soil. Overall, the undrained shear resistance mobilized along the soil-geogrid shear plane was 20 to 30% greater for the novel geogrid than for the conventional geogrid.

**Acknowledgements**

The authors would like to acknowledge the work of Martin Carney, John Kenna and Paul Creaven in performing the tests at the Geotechnical Laboratories, Trinity College Dublin. The paper was written by the first author while on sabbatical leave at the Urban Institute Ireland, University College Dublin.

## References

Almohd, I., Abu-Farsakh, M., Khalid, F., 2006. Geosynthetic reinforcement-cohesive soil interface during pullout. In: Hani, H.T. (Ed.), Proceedings of the 13th Great Lakes Geotechnical and Geoenvironmental Conference, Milwaukee, Wisconsin, USA, pp. 40–49.

ASTM D5321, 2002. Standard test method for determining the coefficient of soil and geosynthetic or geosynthetic and geosynthetic friction by the direct shear method. ASTM International, Pennsylvania, USA.

Bergado, D.T., Shivashankar, R., Sampaco, C.L., Alfaro, M.C., 1991. Behavior of a welded wire wall with poor quality, cohesive-friction backfills on soft Bangkok clay: a case study. Canadian Geotechnical Journal 28, 860–880.

Bergado, D.T., Horpibulsok, S., Ngouchaurieng, P., 2002. Innovative use of geosynthetics for repair of slope failures along irrigation/drainage canals on soft ground. Proceedings of the Seventh International Geosynthetic Conference (IGS-2002), Nice, France.

Bergado, D.T., Ramana, G.V., Sia, H.I., Varun, 2006. Evaluation of interface shear strength of composite liner system and stability analysis for a landfill lining system in Thailand. Geotextiles and Geomembranes 24, 371–393.

Kempton, G.T., Jones, C.J.F.P., Jewell, R.A., Naughton, P.J., 2000. Construction of slopes using cohesive fills and a new innovative geosynthetic material. In: Proceedings of the Second European Geosynthetics Conference, Bologna, pp. 825–828.

Koerner, R.M., 1998. Designing with Geosynthetics, Prentice Hall.

Koutsourais, M.M., Sprague, C.J., Pucetas, R.C., 1991. Interfacial friction study of cap and liner components for landfill design. Geotextiles and Geomembranes 10(5–6), 531–548.

Linear Composites Limited, 2007. Product Data sheets. Available at: www.linear composites.co.uk

Long, M., Menkiti, C.O., 2007. Geotechnical properties of Dublin Boulder Clay. Géotechnique, 57(7), 595–611.

Long, P.V., Bergado, D.T., Abuel-Naga, H.M., 2007. Geosynthetics reinforcement application for tsunami reconstruction: Evaluation of interface parameters with silty sand and weathered clay. Geotextiles and Geomembranes 25, 311–323.

Lorenzo, G.A., Bergado, D.T., Bunthai, W., Hormdee, D., Phothiraksanon, P., 2004. Innovations and performances of PVD and dual function geosynthetic applications. Geotextiles and Geomembranes 22, 75–99.

Nagahara, H., Fujiyama, T., Ishiguro, T., Ohta, H., 2004. FEM analysis of high airport embankment with horizontal drains. Geotextiles and Geomembranes 22, 49–62.

Rowe, R.K., Taechakumthorn, C., Combined effect of PVDs and reinforcement on embankments over rate-sensitive soils. Geotextiles and Geomembranes (in press).

Skipper, J., Follett, B., Menkiti, C.O., Long, M., Clark-Hughes, J., 2005. The engineering geology and characterization of Dublin Boulder Clay. Quarterly J. Engineering Geology and Hydrogeology, 38(2), 171–188.

Tatsuoka, F., Tateyama, M., Mohri, Y., Matsushima, K., 2007. Remedial treatment of soil structures using geosynthetic-reinforcing technology. Geotextiles and Geomembranes 25, 204–220.

Zornberg, J.G., Kang, Y., 2005. Pullout of geosynthetic reinforcement with in-plane drainage capability. In: Proceedings of ASCE Geo-Frontiers Conference, Austin, Texas.

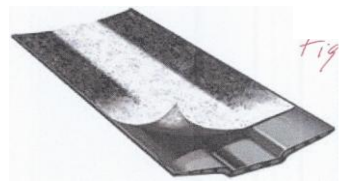

Fig. 1. Novel geogrid (Linear Composites Limited, 2007).

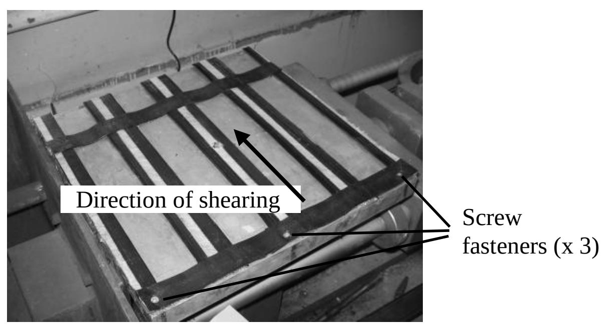


Fig. 2. Novel geogrid straps secured to aluminium plate.

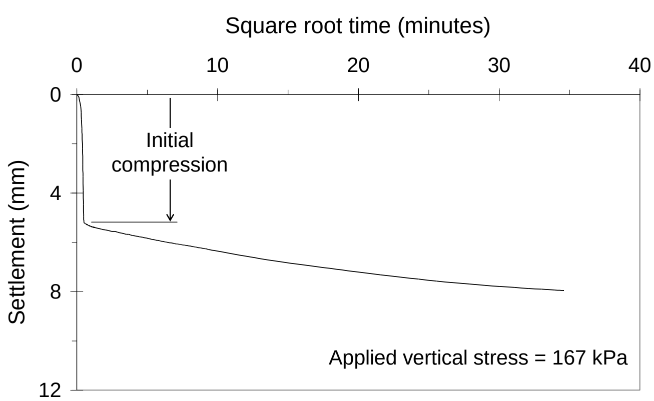


Fig. 3. Consolidation stage of shearbox test on soil-aluminium interface specimen.

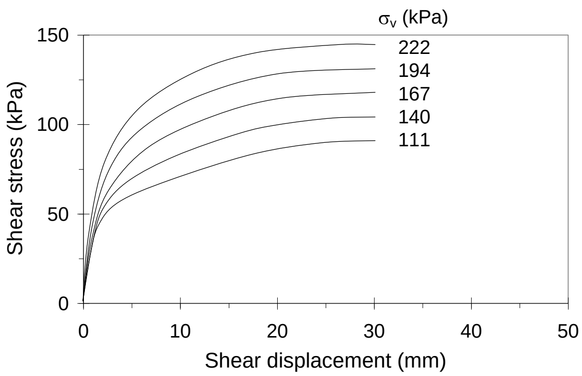


(a) Shear stress versus shear displacement.

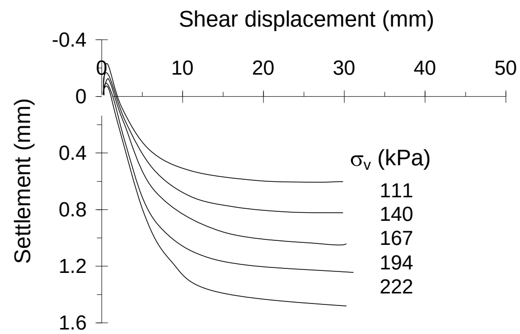


(b) Settlement versus shear displacement.

Fig. 4. Shearbox tests on wet gravely clay material.

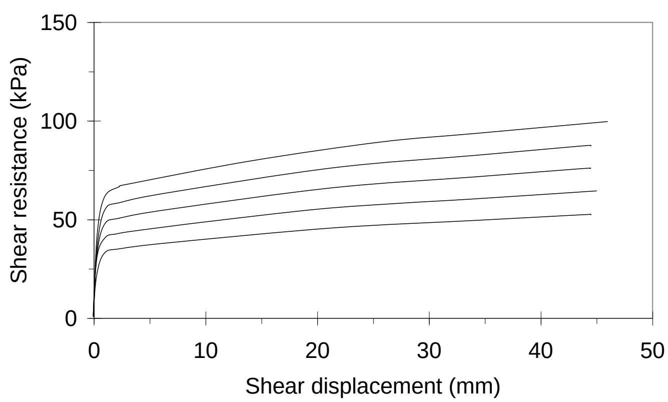


Fig. 5. Shear resistance versus shear displacement for soil-aluminium plate interface.

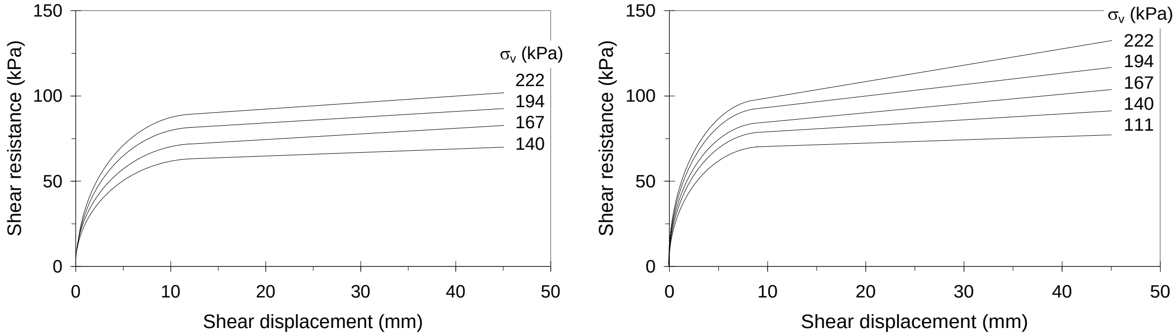


(a) Conventional geogrid. (b) Novel geogrid.

Fig. 6. Shear resistance versus shear displacement for soil-geogrid-plate interfaces.

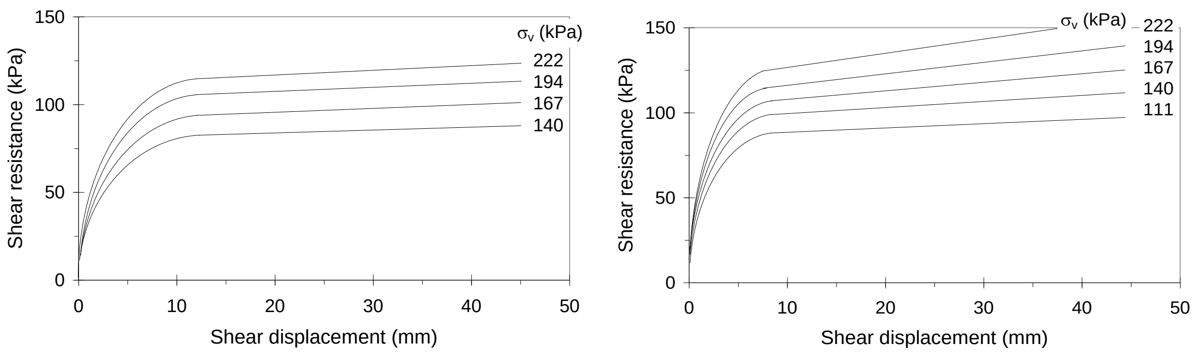


(a) Conventional geogrid. (b) Novel geogrid.

Fig. 7. Interface shear resistance versus shear displacement for soil-geogrid.

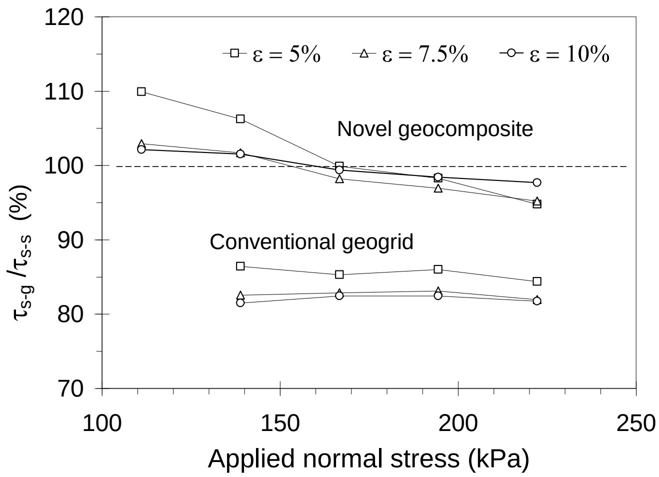


Fig. 8. Normalized undrained interface shear resistance.

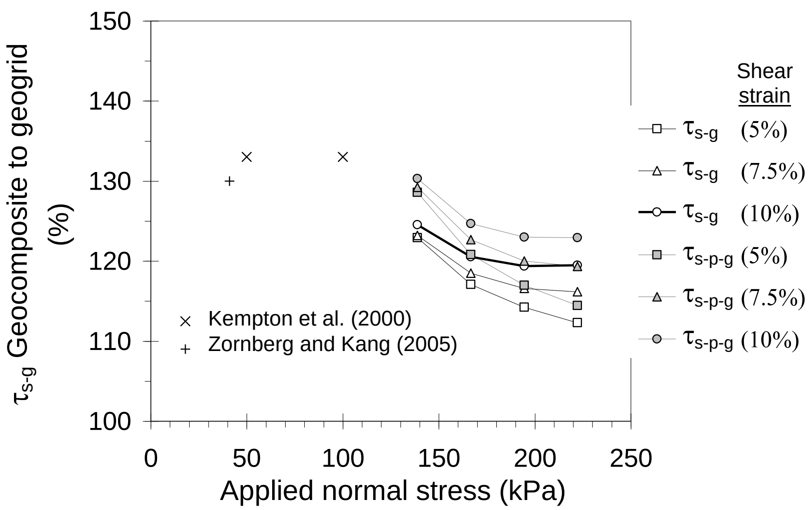


Fig. 9. Enhancement in interface shear resistance achieved for novel geogrid.